



HAL
open science

Contamination levels and habitat use influence Hg accumulation and stable isotope ratios in the European seabass *Dicentrarchus labrax*

Marianna Pinzone, Alice Cransveld, Emmanuel Tessier, Sylvain Bérail, Joseph Schnitzler, Krishna Das, David Amouroux

► To cite this version:

Marianna Pinzone, Alice Cransveld, Emmanuel Tessier, Sylvain Bérail, Joseph Schnitzler, et al.. Contamination levels and habitat use influence Hg accumulation and stable isotope ratios in the European seabass *Dicentrarchus labrax*. *Environmental Pollution*, 2021, 281, pp.117008. 10.1016/j.envpol.2021.117008 . hal-03195726

HAL Id: hal-03195726

<https://hal.science/hal-03195726v1>

Submitted on 26 Nov 2021

HAL is a multi-disciplinary open access archive for the deposit and dissemination of scientific research documents, whether they are published or not. The documents may come from teaching and research institutions in France or abroad, or from public or private research centers.

L'archive ouverte pluridisciplinaire **HAL**, est destinée au dépôt et à la diffusion de documents scientifiques de niveau recherche, publiés ou non, émanant des établissements d'enseignement et de recherche français ou étrangers, des laboratoires publics ou privés.

Journal Pre-proof

Contamination levels and habitat use influence Hg accumulation and stable isotope ratios in the European seabass *Dicentrarchus labrax*

Marianna Pinzone, Alice Cransveld, Emmanuel Tessier, Sylvain Bérail, Joseph Schnitzler, Krishna Das, David Amouroux



PII: S0269-7491(21)00590-X

DOI: <https://doi.org/10.1016/j.envpol.2021.117008>

Reference: ENPO 117008

To appear in: *Environmental Pollution*

Received Date: 21 December 2020

Revised Date: 15 March 2021

Accepted Date: 20 March 2021

Please cite this article as: Pinzone, M., Cransveld, A., Tessier, E., Bérail, S., Schnitzler, J., Das, K., Amouroux, D., Contamination levels and habitat use influence Hg accumulation and stable isotope ratios in the European seabass *Dicentrarchus labrax*, *Environmental Pollution*, <https://doi.org/10.1016/j.envpol.2021.117008>.

This is a PDF file of an article that has undergone enhancements after acceptance, such as the addition of a cover page and metadata, and formatting for readability, but it is not yet the definitive version of record. This version will undergo additional copyediting, typesetting and review before it is published in its final form, but we are providing this version to give early visibility of the article. Please note that, during the production process, errors may be discovered which could affect the content, and all legal disclaimers that apply to the journal pertain.

© 2021 Elsevier Ltd. All rights reserved.

Contamination levels and habitat use influence Hg accumulation and stable isotopes in the European seabass

Dicentrarchus labrax.

Marianna Pinzone^{a*}, Alice Cransveld^{a*}, Emmanuel Tessier^b, Sylvain Bérail^b, Joseph
Schnitzler^{a,c}, Krishna Das^a, David Amouroux^b.

*Both authors contributed equally to the work

^aFreshwater and Oceanic sciences Unit of reSearch (FOCUS), Laboratory of Oceanology, University of Liège B6c Allée du 6 Août, 4000 Liège, Belgium

^bUniversité de Pau et des Pays de l'Adour, E2S UPPA, CNRS, Institut des Sciences Analytiques et de Physico-chimie pour l'Environnement et les matériaux (IPREM), Technopôle Hélioparc, 2 Avenue Pierre Angot, 64053 Pau Cedex 09, France

^cInstitute for Terrestrial and Aquatic Wildlife Research, University of Veterinary Medicine Hannover, Foundation, 25761 Büsum, Schleswig-Holstein, Germany.

- Marianna Pinzone: Data curation, Writing – review and editing, Visualization, Formal analysis, Conceptualization
- Alice Cransveld: Conceptualization, Methodology, Formal analysis, Writing – original draft
- Emmanuel Tessier: Analytical measurements, Software, Validation
- Sylvain Bérail: Resources, Analytical measurements, Validation
- Joseph Schnitzler: Supervision, Formal analysis, Validation
- Krishna Das: Resources, Project administration, Funding acquisition, Supervision
- David Amouroux: Resources, Supervision, Validation

1 **Contamination levels and habitat use influence Hg**
2 **accumulation and stable isotope ratios in the European**
3 **seabass *Dicentrarchus labrax*.**

4
5 Marianna Pinzone^{a*}, Alice Cransveld^{a*}, Emmanuel Tessier^b, Sylvain Bérail^b, Joseph
6 Schnitzler^{a,c} Krishna Das^a, David Amouroux^b.

7 *Both authors contributed equally to the work

8
9 ^aFreshwater and Oceanic sciences Unit of reSearch (FOCUS), Laboratory of Oceanology,
10 University of Liège, B6c Allée du 6 Août, 4000 Liège, Belgium

11 ^bUniversité de Pau et des Pays de l'Adour, E2S UPPA, CNRS, Institut des Sciences
12 Analytiques et de Physico-chimie pour l'Environnement et les matériaux (IPREM),
13 Technopôle Helioparc, 2 Avenue Pierre Angot, 64053 Pau Cedex 09, France

14 ^cInstitute for Terrestrial and Aquatic Wildlife Research, University of Veterinary Medicine of
15 Hannover, Foundation, Werftstraße 6, 25761 Büsum, Schleswig-Holstein, Germany.

16
17 Corresponding author: Krishna.das@uliege.be

18

19 Abstract

20 Hg accumulation in marine organisms depends strongly on *in situ* water or sediment
21 biogeochemistry and levels of Hg pollution. To predict the rates of Hg exposure in human
22 communities, it is important to understand Hg assimilation and processing within
23 commercially harvested marine fish, like the European seabass *Dicentrarchus labrax*.
24 Previously, values of $\Delta^{199}\text{Hg}$ and $\delta^{202}\text{Hg}$ in muscle tissue successfully discriminated between
25 seven populations of European seabass. In the present study, a multi-tissue approach was
26 developed to assess the underlying processes behind such discrimination.

27 We determined total Hg content (THg), the proportion of monomethyl-Hg (%MeHg), and Hg
28 isotopic composition (e.g. $\Delta^{199}\text{Hg}$ and $\delta^{202}\text{Hg}$) in seabass liver. We compared this to the
29 previously published data on muscle tissue and local anthropogenic Hg inputs.

30 The first important finding of this study showed an increase of both %MeHg and $\delta^{202}\text{Hg}$
31 values in muscle compared to liver in all populations, suggesting the occurrence of internal
32 MeHg demethylation in seabass. This is the first evidence of such a process occurring in this
33 species. Values for mass-dependent (MDF, $\delta^{202}\text{Hg}$) and mass-independent (MIF, $\Delta^{199}\text{Hg}$)
34 isotopic fractionation in liver and muscle accorded with data observed in estuarine fish (MDF,
35 0-1‰ and MIF, 0-0.7‰). Black Sea seabass stood out from other regions, presenting higher
36 MIF values ($\approx 1.5\%$) in muscle and very low MDF ($\approx -1\%$) in liver. This second finding
37 suggests that under low Hg bioaccumulation, Hg isotopic composition may allow the
38 detection of a shift in the habitat use of juvenile fish, such as for first-year Black Sea seabass.
39 Our study supports the multi-tissue approach as a valid tool for refining the analysis of Hg
40 sourcing and metabolism in a marine fish. The study's major outcome indicates that Hg levels
41 of pollution and fish foraging location are the main factors influencing Hg species
42 accumulation and isotopic fractionation in the organisms.

43

44 **Keywords:** multi-tissue; stable isotopes; seabass; demethylation; contamination level

45

46 **Main finding:** Our novel results support the occurrence of *in vivo* MeHg demethylation in

47 European seabass. They also show that, in this fish, environmental levels of Hg pollution

48 influence demethylation rates and inter-organ MDF.

Journal Pre-proof

49 **Introduction**

50 Monomethyl-Hg (MeHg), the most toxic form of Hg, is readily bioavailable in the marine
51 environment and bioaccumulates in the food web (Hong et al., 2012; Lang et al., 2017;
52 Mozaffarian and Rimm, 2008; Renzoni et al., 1998; UNEP, 2018, 2013). Several processes
53 modulate MeHg bioavailability (Du et al., 2019). In surface waters, sunlight radiation can
54 control the degradation of methylated Hg species. Several mechanisms are proposed to cause
55 MeHg photodegradation (Luo et al., 2020). It is generally recognized that this process is
56 induced by ultraviolet light (UV-A and UV-B, 280-400 nm) (Lehnher and St. Louis, 2009)
57 and controlled by the type and abundance of MeHg-binding ligands (e.g. OH⁻, ¹O₂, DOM,
58 organic thiols or chloride complexes) in the water column (Luo et al., 2020; Zhang and Hsu-
59 kim, 2010). In deeper layers, MeHg is mostly processed by microbial activity, either in the
60 aphotic water column during microbial remineralization of settling organic matter, or in
61 anoxic conditions at the sea bottom (Gworek et al., 2016; Li et al., 2016; Mason et al., 2001;
62 Sunderland et al., 2010). Iron- and sulfur-reducing bacteria (IRB and SRB, respectively) as
63 well as methanogens are the main groups of prokaryotes responsible for Hg processing in
64 anoxic conditions (Bystrom, 2008; Lu et al., 2016; Regnell and Watras, 2019).

65 Consequently, local climatic and oceanographic features, combined with growing
66 anthropogenic activities, might alter the complex Hg cycle, with unknown consequences for
67 its marine life. Apex predators such as marine mammals, seabirds or carnivorous fish can
68 accumulate extremely high levels of Hg, being at the top of marine food webs (Sonke et al.,
69 2013). For this reason, understanding Hg uptake and accumulation in these animals is a
70 priority. Such urgency is also related to the fact that most species of edible carnivorous fish
71 (tuna, cod, seabass etc.) are commonly consumed by humans (Serrell et al., 2012).

72 Recently, the use of stable isotopes of Hg was proven useful for discriminating
73 between potential Hg sources and accumulation in aquatic habitats (Bergquist and Blum,

74 2009; Cransveld et al., 2017; Gantner et al., 2009; Gehrke et al., 2011; Kwon et al., 2014a;
75 Perrot et al., 2010; Point et al., 2011; Senn et al., 2010; Sherman and Blum, 2013; Yin et al.,
76 2016). The seven stable isotopes of Hg ($Z = 196, 198, 199, 200, 201, 202$ and 204) can
77 undergo mass-dependent fractionation (MDF) and mass-independent fractionation (MIF)
78 (Bergquist and Blum, 2009). MDF (mostly represented by $\delta^{202}\text{Hg}$) occurs during a variety of
79 chemical, physical and biological reactions, and has been used to detail the processes
80 controlling Hg transport, transformation and bioaccumulation (Bergquist and Blum, 2009).
81 More specifically, MDF can be used to trace Hg transfer from the environment throughout the
82 food web (Tsui et al., 2019). The latest constraints to the interpretation of MDF data include
83 its quantification at higher trophic levels, where fractionation rates are complicated by
84 biotransformation processes occurring within the organisms (e.g. demethylation) (Tsui et al.,
85 2019). MIF is not modified throughout the food web and thus provides a unique fingerprint of
86 primary Hg sources in the marine environment (Obrist et al., 2018). The occurrence of MIF
87 (represented mostly by $\Delta^{199}\text{Hg}$ and $\Delta^{201}\text{Hg}$ values) has been attributed to all photochemical
88 reactions, such as photochemical reduction of Hg^{2+} (Bergquist and Blum, 2007), and
89 photodemethylation of DOM-associated MeHg in both the water column (Chandan et al.,
90 2015) and marine phytoplankton cells (Kritee et al., 2018). Finally, even-mass isotopes
91 ($\Delta^{200}\text{Hg}$, $\Delta^{204}\text{Hg}$) are dependent on the atmospheric cycle of Hg, discriminating for example
92 between precipitation sources (e.g. snow vs. rain) (Gratz et al., 2010; Sherman et al., 2010).

93 We recently measured MDF and MIF values in seabass muscle (*Dicentrarchus labrax*)
94 to discriminate between different sub-populations in Europe and in the Black Sea (Cransveld
95 et al., 2017). We highlighted a large heterogeneity in Hg MDF and MIF between the seven
96 sampling regions, and suggested hepatic MeHg demethylation or different Hg sourcing as
97 potential causes (Cransveld et al., 2017). However, the exclusive use of muscle as the
98 monitoring tissue did not allow more extensive interpretation.

99 Indeed, while Hg monitoring studies often focus on muscle, the analysis of Hg
100 isotopes and speciation in liver can bring additional perspectives (Tsui et al., 2019). Each
101 tissue indeed exhibits specific concentrations and proportions of Hg species (Mieiro et al.,
102 2011; Pentreath, 1976), depending on several factors: tissue composition (proteins, lipids,
103 carbohydrates), turnover rate, and the food regime of fish (Jardine et al., 2006; Maury-Brachet
104 et al., 2006; Perga and Gerdeaux, 2005; Wang and Wong, 2003). For this reason, the
105 inclusion of more tissues in the assessment of Hg stable isotopes in a single organism was
106 proposed as a valid and necessary approach that may offer a more comprehensive picture of
107 the dynamics of contaminant uptake (Jardine et al., 2006; Tsui et al., 2019) and internal
108 processing by marine organisms (Kwon et al., 2016, 2012). In this regard, liver is the key
109 tissue. In marine mammals, aquatic birds and some fish species, the liver is demonstrated to
110 act as detoxifying organ (Booth and Zeller, 2005; Eagles-Smith et al., 2009; Feng et al., 2015;
111 Gonzalez et al., 2005; Wagemann et al., 1998). Thus, the combination of stable isotope
112 analysis in both muscle and liver of marine predators could allow a complete understanding
113 of MeHg sources and processing in both wildlife and the wider environment.

114 Therefore, to understand Hg sources and organotropism of this species around Europe,
115 in this study we compared THg, %MeHg and Hg isotope composition (MIF and MDF) in the
116 liver of wild seabass *Dicentrarchus labrax* with previously published muscle data (Cransveld
117 et al., 2017). Specifically, we wanted to test three distinct hypotheses: (1) The use of a multi-
118 tissue approach improves isotopic tracing of Hg biogeochemical processes and sources
119 between natural ecosystems, in comparison with the singular analysis of muscle; (2) MeHg
120 demethylation may occur in seabass liver and its rates can be dependent on the extent of local
121 mercury pollution; (3) the peculiar biogeochemical settings of each sampling site may
122 determine the particular sourcing of MeHg in local seabass.

123

124 **Materials and method**

125 **Sample collection**

126 Sampling of the seabass *Dicentrarchus labrax* used in the present study has been described
127 previously (Cransveld et al., 2017). All the biometric information available for the sampled
128 fish is summarized in Table 1. All fish were juveniles, sampled at their nursery sites. Fish
129 were collected between 2012 and 2014 from seven coastal sites throughout Europe: the North
130 Sea (NS), the Northern Aegean Sea (AES), the Seine Estuary (SE), the Northern Adriatic Sea
131 (NAS), the Turkish coast of the Black Sea (BS), and two different sites at the Ria de Aveiro
132 in Portugal (a “reference” site and a “contaminated” site – RAR and RAC respectively).
133 These sites are subjected to different levels of Hg pollution because of their specific industrial
134 origin. Details about each site are given in Table 1 and in the Supporting Information of
135 Cransveld *et al.* (2017). Sites were separated into “low”, “moderate” and “highly” polluted
136 categories, based on the statistical differences published on muscle concentrations (Cransveld
137 et al., 2017). Figure S1 shows these three groups as *a*, *b* and *c*. After sampling, fish were kept
138 in freezers at -20°C. Prior to dissection, fish were measured and weighed. Liver was sampled,
139 freeze-dried and ground into powder.

140 **Analyses**

141 THg concentrations were determined in the liver of fish through the use of a Milestone Direct
142 Mercury Analyzer 80 (Habran et al., 2012), using the US EPA Method 7473, validated for
143 solid samples. THg concentrations are expressed as ng.g⁻¹ dry weight (DW). Quality
144 assurance methods included measuring blanks (HCl 1%), standard solutions (100 ng Hg.ml⁻¹),
145 triplicates of samples, and certified reference material NRC-DORM-2 (certified T-Hg value =
146 4640 ± 260 ng.g⁻¹ dw). CRM recovery percentages ranged from 89% to 110% (Table S1).
147 MeHg concentrations were determined by isotope dilution-gas chromatography, inductively-
148 coupled-plasma mass spectrometer (ID-GC-ICP-MS), following microwave-assisted

149 extraction and aqueous phase derivatization, as detailed elsewhere (Cransveld et al., 2017;
150 Rodríguez Martín-Doimeadios et al., 2002). For the extraction, between 50-100 mg of the
151 liver sample was weighed. BCR CRM-464 (tuna fish muscle certified for MeHg and THg
152 concentration) and DOLT-4 (dogfish liver) were used as reference materials. Certified and
153 obtained THg and MeHg values are shown in Table S2. All solutions were prepared using
154 ultrapure water (18M Ω cm, Millipore). Trace Metal Grade acids HNO₃ and HCl from Fisher
155 Scientific (Illkirch, France) and ultrapure H₂O₂ (67-70%, ULTREX® II, J.T.Baker) were used
156 for the preparation of all the samples, standards and blanks. Between 20 and 570 mg of liver
157 samples were mineralized in quartz vials with trace metal grade nitric acid (HNO₃), using a
158 HPA High Pressure Asher (Anton Paar, Austria). Then, ultrapure hydrogen peroxide (H₂O₂)
159 was added, and samples went through a digestion process for three more hours on a hot block
160 (80°C) to ensure full mineralization of organic matter. The samples were then diluted to
161 obtain a final Hg concentration of 1 ng.g⁻¹ in an acid solution, which was adjusted to contain
162 10% HNO₃ and 2% HCl. Blanks were prepared by pouring nitric acid in vials, without
163 samples. CRM recovery percentages ranged from 74% to 94% (Table S2).

164 Mercury isotopic composition analysis was performed using cold vapor generation
165 (CVG) with multi-collector-inductively coupled plasma-mass spectrometer (MC-ICP-MS, Nu
166 Instruments) (Cransveld et al., 2017). A desolvation / nebulization system from Nu
167 Instrument was used to introduce NIST-SRM-997 thallium for instrumental mass-bias
168 correction using the exponential fractionation law. Reference material NIST RM 8610
169 (former UM-Almaden), ERM-CE-464 and DOLT-4 were used as secondary standards. The
170 resulting Hg isotopic composition is presented in Table S3.

171 We used a standard-sample bracketing system to calculate δ values (in ‰) relative to
172 the reference standard NIST SRM 3133 mercury spectrometric solution. Isotope ¹⁹⁸Hg was

173 used as the reference for ratio determination of all other Hg isotopes, using the following
 174 equations:

$$\delta^{xxx}\text{Hg} = \left[\frac{(\text{xxxHg}/^{198}\text{Hg})_{\text{sample}}}{(\text{xxxHg}/^{198}\text{Hg})_{\text{NIST 3133}}} - 1 \right] \times 1000$$

175 MDF processes will be represented by $\delta^{202}\text{Hg}$ values. MIF processes will be calculated and
 176 represented as follows for odd (1 & 2) and even (3 & 4) isotopes:

$$(1) \quad \Delta^{199}\text{Hg} = \delta^{199}\text{Hg}_{\text{observed}} - \delta^{199}\text{Hg}_{\text{predicted}} = \delta^{199}\text{Hg}_{\text{observed}} - (\delta^{202}\text{Hg} \times 0.252)$$

$$(2) \quad \Delta^{201}\text{Hg} = \delta^{201}\text{Hg}_{\text{observed}} - \delta^{201}\text{Hg}_{\text{predicted}} = \delta^{201}\text{Hg}_{\text{observed}} - (\delta^{202}\text{Hg} \times 0.752)$$

$$(3) \quad \Delta^{200}\text{Hg} = \delta^{200}\text{Hg}_{\text{observed}} - \delta^{200}\text{Hg}_{\text{predicted}} = \delta^{200}\text{Hg}_{\text{observed}} - (\delta^{202}\text{Hg} \times 0.502)$$

$$(4) \quad \Delta^{204}\text{Hg} = \delta^{204}\text{Hg}_{\text{observed}} - \delta^{204}\text{Hg}_{\text{predicted}} = \delta^{204}\text{Hg}_{\text{observed}} - (\delta^{202}\text{Hg} \times 1.493)$$

177 A more detailed description of Hg speciation and isotope analysis, including quality assurance
 178 and method validation, can be found in the Supporting Information of this work and in
 179 previous literature (Cransveld et al. 2017; Renedo et al. 2018).

180 **Statistics**

181 Since the sampling size was small ($n \leq 12$) for each sampling location, we used non-
 182 parametric tests for statistical analyses. Statistical significance was set at $\alpha = 0.01$ (instead of
 183 0.05). Differences between groups with p -values between 0.05 and 0.01 were reported in the
 184 results but not interpreted as effective. To test variance amongst sampling sites, we used the
 185 non-parametric Kruskal-Wallis (K-W) for each parameter separately. We used the
 186 Spearman's ρ to correlate concentrations and isotopic values. Finally, to test the difference
 187 between variables measured in muscle and in liver, we used the paired samples Wilcoxon test.

188

189 **Results**

190 **THg and MeHg concentrations**

191 Concentrations of THg in muscle and liver differed significantly between sampling sites (K-
192 W; $H = 50.81$; $p < 0.0001$ and $H = 46.60$; $p < 0.0001$) (Table 2). These were separated into
193 three groups: the most contaminated NAS and RAC, the intermediate RAR, NS and SE, and
194 the least contaminated AES and BS (Figure S1). In liver, such differences were less
195 important, but THg and MeHg concentrations followed the same profile (Figure S1-Right and
196 Table 2).

197 Liver %MeHg differed significantly between sampling sites (K-W; $H = 41.00$; $p < 0.0001$),
198 ranging from 7% in BS to 82% in NAS (Figure S2b). For the whole dataset ($n = 62$), THg was
199 moderately correlated to %MeHg ($r = 0.51$; $p = 0.0001$). In muscle, %MeHg varied less, with
200 a significant difference observed only between SE and NAS and AES (K-W; $H = 36.91$; $p <$
201 0.0001). Percentage values ranged between 71% in NAS and 93% in SE (Figure S2a). No
202 correlation was found between the %MeHg in muscle and THg levels among regions
203 (Spearman; $r = 0.13$; $p = 0.324$).

204

205 **Hg stable isotope composition**

206 Hepatic $\delta^{202}\text{Hg}$ and $\Delta^{199}\text{Hg}$ values varied significantly between sampling locations (K-W; $H =$
207 50.69 ; $p < 0.0001$ and $H = 38.55$; $p < 0.0001$, respectively) (Table 2). There was strong
208 correlation between $\Delta^{199}\text{Hg}$ and $\Delta^{201}\text{Hg}$ (Spearman; $r = 0.95$; $p < 0.0001$) for all sites, and the
209 value of the slope of the regression line was 1.30 ± 0.02 (Figure 1a). A positive correlation
210 between $\Delta^{199}\text{Hg}$ and $\delta^{202}\text{Hg}$ values was found only for SE ($p = 0.001$, $\rho = 0.661$), BS ($p =$
211 0.005 , $\rho = 0.628$) and RAC ($p = 0.016$, $\rho = 0.530$) (Figure 1b). Only BS fish showed a
212 positive correlation between $\Delta^{199}\text{Hg}$ and $\delta^{202}\text{Hg}$ values and %MeHg in both tissues
213 (respectively: $p < 0.0001$, $\rho = 0.767$ and $p = 0.0013$, $\rho = 0.698$).

214 Only a weak difference was observed in hepatic $\Delta^{200}\text{Hg}$ values (Figure S3a; K-W, $H = 14.33$

215 and $p = 0.023$), with AES presenting higher even-MIF than RAC and SE. $\Delta^{204}\text{Hg}$ values
216 differed slightly more (Figure S3b; K-W, $H = 19.83$ and $p = 0.003$) with RAC presenting
217 significantly smaller MIF than RAR and SE. The great variation found in even-MIF values
218 did not allow us to discriminate between specific atmospheric sources in seabass populations
219 and will not be discussed further. Raw data and a short discussion are given in the Supporting
220 Information (Section S2.a, Table S4, Figure S3a and b).

221 When compared with muscle results published in Cransveld *et al.* (2017), the difference
222 between $\delta^{202}\text{Hg}_{\text{muscle}}$ and $\delta^{202}\text{Hg}_{\text{liver}}$ ranged from 0.04‰ in NAS to 1.08‰ in BS. $\delta^{202}\text{Hg}$
223 values differed significantly between the two tissues only in BS seabass (K-W, $H = 84.9$, $p =$
224 0.003). The difference between $\Delta^{199}\text{Hg}_{\text{muscle}}$ and $\Delta^{199}\text{Hg}_{\text{liver}}$ went from -0.02‰ in NAS to
225 1.13‰ in BS. As before, $\Delta^{199}\text{Hg}$ values differed only in BS seabass (K-W, $H = 95.5$, $p <$
226 0.0001). $\delta^{15}\text{N}$, $\delta^{13}\text{C}$ values and trophic position (TL) in the different seabass populations were
227 presented elsewhere (Cransveld *et al.*, 2017). No correlation was found between carbon and
228 nitrogen isotope ratios in seabass muscle and %MeHg in liver. For this reason, we do not
229 discuss these results further. More details can be found in paragraph S2.b.

230

231 **Discussion**

232 **Evidence of Hg demethylation in seabass across Europe**

233 The lowest THg muscle and liver concentrations were observed in Greece and the Black Sea
234 (AES and BS sites), while the highest concentrations were measured in the North Adriatic Sea
235 and Ria d'Aveiro (NAS and RAC sites; Table 2). Liver %MeHg ranged from 7-10% in BS,
236 30-40% in the contaminated area of RAC, and up to 70% in NS, SE and AES. On the other
237 hand, muscle %MeHg was constant around 80-90% across all sites (Cransveld *et al.*, 2017).
238 The different MeHg profile between muscle and liver is in accordance with previous literature
239 and the role that these two tissues have in the fish body (Mieiro *et al.*, 2009). Muscle is often

240 described as the final Hg storage tissue in marine vertebrates, where dietary MeHg is
241 accumulated at a high rate and not metabolized further (Oliveira Ribeiro et al., 1999). This is
242 why %MeHg remains constant. Instead, the extremely variable proportions of MeHg
243 displayed by liver are thought to be an expression of the protective role of this organ (Mieiro
244 et al., 2011; Oliveira Ribeiro et al., 1999). Indeed, in this organ, dietary MeHg binds with
245 Selenium (Se) and is transformed into an inert tiemannite complex (HgSe) (Sonne et al.,
246 2009). In this way, Hg is locally accumulated in a less toxic and non-available inorganic
247 form. Through the application of Hg stable isotope ratios, there is increasing evidence that the
248 liver acts as a Hg detoxification center in fish, as it does in marine mammals or seabirds
249 (Renedo et al., 2021; Wang et al., 2013, 2017).

250 Hg stable isotopes can undergo MDF during uptake and metabolism of Hg within the
251 organisms (transfer, transformation and excretion) (Li et al., 2020). Important Hg MDF
252 related to MeHg demethylation is now also broadly accepted to occur in fish (Man et al.,
253 2019; Wang and Tan, 2019). MeHg demethylation causing MDF preferentially involves
254 lighter Hg isotopes and generates newly formed iHg, having a lower $\delta^{202}\text{Hg}$ (Perrot et al.,
255 2015). The remaining non de-methylated MeHg will then have a higher $\delta^{202}\text{Hg}$ compared to
256 the initially bioaccumulated MeHg (Perrot et al., 2015). Because most iHg is excreted, the
257 fractionation (MDF) caused by demethylation is probably more observable in MeHg-rich
258 tissues like muscle (Gehrke et al., 2011; Kwon et al., 2014a; Sherman and Blum, 2013). Since
259 liver is the center of *in vivo* demethylation and therefore contains a lower proportion of
260 MeHg, it will display lower $\delta^{202}\text{Hg}$ values than muscle. Consequently, a large shift in $\delta^{202}\text{Hg}$
261 values and %MeHg between muscle and liver tissues of seabass could infer the occurrence of
262 MeHg demethylation in the liver of the fish (Wang et al., 2013). All our sampling areas
263 showed a significant difference in %MeHg between muscle and liver (Figure 2). For $\delta^{202}\text{Hg}$
264 values the difference was less striking. A significant statistical difference was found only in

265 BS fish (Figure 2a); nevertheless, MDF was higher in muscle than liver for all sites. This
266 result suggests that MeHg demethylation might indeed be occurring in the livers of European
267 seabass. This is the first evidence that such a process might occur in this fish species, and
268 specifically in juvenile individuals. This represents a very important result, considering
269 existing conflicting literatures about MeHg demethylation capacity in fish organisms.

270 Regarding the hypothesis that *in vivo* demethylation was the only process affecting MDF in
271 seabass, we should expect to have the same $\delta^{202}\text{Hg}$ difference between muscle and liver
272 across all sites. However, this was not the case since BS seabass presented a much larger
273 $\delta^{202}\text{Hg}$ difference than the other sites. Cransveld et al. (2017) proposed that the particular Hg
274 isotopic composition of the BS subpopulation could be explained by the presence of MeHg
275 demethylation (Cransveld et al., 2017). Our findings have shown that such a process is
276 occurring in all the sampled seabass. Therefore, one possibility is that BS seabass might
277 demethylate MeHg at higher rates, which would lead to a larger difference in $\delta^{202}\text{Hg}$ values
278 between muscle and liver. Several processes might determine higher rates of Hg
279 organotropism and demethylation: the levels of local Hg pollution, fish age, exposure to
280 different sources of Hg from the environment, fish diet, and finally the particular
281 biogeochemistry of the studied area, which affects local Hg cycling in the marine
282 environment. These factors will be analyzed one-by-one in the following paragraphs.

283

284 **A higher extent of local Hg pollution hides inter-organ Hg MDF**

285 Previous studies have shown that in highly polluted systems, liver can accumulate iHg
286 directly from the environment, through the gills or the skin (Feng et al., 2015). For this
287 reason, hepatic Hg levels and detoxification rates might be affected by levels of Hg pollution
288 in the environment (Guilherme et al., 2008). Indeed, in areas with higher anthropogenic
289 pollution discharge, studies have demonstrated a decrease in %MeHg in fish liver (Rua-Ibarz

290 et al., 2019). This seems to be primarily due to two different processes: first, the exposure to
291 higher levels of environmental iHg deriving from anthropogenic activities leads to higher
292 accumulation of this Hg species in the liver (Gentès et al., 2015); secondly, the higher Hg
293 intake in the animal (through diet or gills) leads to higher hepatic MeHg demethylation rates
294 (Cizdziel et al., 2003; Perrot et al., 2015). If this were true, we would observe a larger
295 difference in %MeHg between muscle and liver tissues in highly polluted areas compared to
296 unpolluted ones. In the same way, because of the depletion in ^{202}Hg observed during
297 demethylation of MeHg in liver, we should get a higher difference between muscle $\delta^{202}\text{Hg}$
298 and liver $\delta^{202}\text{Hg}$ in seabass collected in highly polluted areas.

299 In our study, the profile of %MeHg in the liver of European seabass indeed reflects the
300 history of Hg contamination between our sampling sites, with moderately polluted areas such
301 as NS and SE presenting $\approx 70\%$ of MeHg in liver and the highly polluted ones like RAC and
302 NAS presenting $\approx 40\%$ of MeHg. The Ria d'Aveiro (RAC) has been subjected to Hg effluents
303 from a chlor-alkali plant for almost five decades (1950-1994). Today, very high Hg
304 concentrations can still be found in bottom sediments (Coelho et al., 2005; Mieiro et al.,
305 2011). NAS samples were collected in the lagoon of Marano and Grado in the Gulf of Trieste.
306 This area is known to have a long history of Hg pollution, due to the presence of the Idrija
307 mercury mine and chlor-alkali plants active between 1949-1984 (Foucher et al., 2009;
308 Živković et al., 2017). On the other hand, AES samples were collected in the Agiasma
309 lagoon, which is today a RAMSAR protected area (Table 1). This region is usually associated
310 with quite low levels of Hg (Christophoridis et al., 2007). This second result suggests that
311 mercury accumulation and organotropism in European seabass from NAS, NS, SE, AES,
312 RAR and RAC is governed by the extent of local pollution, and controlled by the protective
313 role played by the liver. However, this cannot apply to BS, which contrasted with all other
314 sites, showing the lowest THg levels and %MeHg in liver (around 7%, Table 2). Moreover,

315 the difference between $\delta^{202}\text{Hg}$ in muscle and liver was found to be the greatest in BS fish,
316 followed by the second least polluted site of AES. Conversely, the moderately and highly
317 polluted areas did not show any significant differences (Figure S4). This result is in contrast
318 with our previous observation of larger inter-organ MDF in more polluted areas, supporting
319 the idea that the larger extent of BS MeHg hepatic demethylation is not governed by Hg
320 pollution.

321 A possible factor influencing the rate of MeHg demethylation, and therefore Hg MDF, is fish
322 age. BS seabass were one year old, while in NAS, SE, NS and AES we sampled two- and
323 three-year-old fish (Cransveld et al., 2017). Several studies have demonstrated how the
324 detoxifying activity of liver can change during the lifetime of an organism, due to metabolic
325 shifts linked with growth rates (Le Croizier et al., 2020). Younger fast-growing animals have
326 higher metabolic rates, which lead to faster isotopic routing and contaminant accumulation
327 (Pinzone et al., 2017). Therefore, the large $\delta^{202}\text{Hg}$ tissue offset in BS might be due to the fact
328 that these fish are younger than SE, NS, AES and NAS ones. However, this does not apply to
329 RAC and RAR fish, which are also one year old, but do not show the same large $\delta^{202}\text{Hg}$ offset
330 between tissues (Figure S4).

331 The similar age of NAS or RAC and BS fish therefore excludes attributing the difference in
332 the extent of MeHg demethylation to growing rates. This, in addition to the inconsistency of
333 BS seabass presenting both the highest inter-organ MDF and lowest Hg pollution, shows that
334 while the levels of environmental Hg pollution generally influence Hg organotropism in this
335 species, the inter-organ Hg MDF variability might not result from a difference in
336 demethylation rates across sites.

337 It could instead be proposed that the Hg isotopic variability observed in our seven seabass
338 subpopulations results from the extreme difference in Hg levels between the most polluted
339 sites NAS and RAC and the least polluted sites of BS and AES. Indeed, in very contaminated

340 areas, seabass might be exposed to levels of dietary MeHg so elevated that it can saturate the
341 organism (Feng et al., 2015). In this situation, differences in Hg levels and isotopic values
342 between organs might be masked (Havelková et al., 2008). This could be the reason for the
343 absence of inter-organ MDF offset in seabass from NAS or RAC. On the other hand, we can
344 readily discriminate Hg inter-organ transfer and demethylation processes in BS seabass
345 because of the limited Hg pollution in the area.

346

347 **$\Delta^{199}\text{Hg}$ MIF inter-tissue comparison indicates same Hg origin for all seabass**
348 **populations.**

349 If Hg pollution was the only factor influencing seabass Hg isotopic composition, we would
350 observe the same pattern in both AES and BS, because of their similar Hg levels. However, it
351 is worth remembering that BS seabass were the only ones in which the $\delta^{202}\text{Hg}$ offset between
352 the muscle and liver was significantly different. When comparing BS fish with the rest of the
353 sampling sites, we can observe that the large difference in $\delta^{202}\text{Hg}$ is caused by significantly
354 lower values ($\approx -1\%$) in liver tissue compared to the other regions (Figure 2a). Muscle $\delta^{202}\text{Hg}$
355 values are instead similar to other regions, in accordance with previous findings in estuarine
356 biota (Kwon et al., 2014b). Beside metabolic processes, Hg stable isotope MDF can occur
357 during a variety of biotic and dark abiotic reactions, such as microbial reduction of iHg
358 ($\delta^{202}\text{Hg} \approx -1.6\%$) or microbial demethylation of MeHg ($\delta^{202}\text{Hg} \approx -0.4\%$) (Tsui et al., 2019).
359 Therefore, the negative MDF signature of BS fish could reflect the local marine Hg
360 biochemical cycle. However, the great variability of processes causing MDF complicates the
361 interpretation of our data.

362 Hg stable isotope MIF is caused by photochemical processes in the environment and is not
363 modified by *in vivo* metabolism (Blum et al., 2014). For this reason, it can be used more
364 easily to trace Hg sources in marine fish (Zheng and Hintelmann, 2009). $\Delta^{199}\text{Hg}$ values

365 should not differ between muscle and liver tissues when fish are exposed to Hg originating
366 from a single source point (Perrot et al., 2010). As expected, we found no statistical difference
367 between liver and muscle $\Delta^{199}\text{Hg}$ values from all sites, again with the single exception of BS,
368 whose muscle $\Delta^{199}\text{Hg}$ values were $> 1\text{‰}$ higher than those for liver (Figure 2b). These values
369 are also higher than $\Delta^{199}\text{Hg}$ found in all the other sites. As for $\delta^{202}\text{Hg}$ values, BS MIF
370 signature was the only one to correlate positively with %MeHg between tissues, confirming
371 again that both MDF and MIF in this population depends on Hg species distribution between
372 muscle and liver.

373 A first hypothesis is that the two tissues represent two separate endmembers of Hg in this
374 population. In fish, the liver accumulates Hg in three forms: MeHg from the diet, iHg from
375 demethylated MeHg, and environmental iHg. While more than 95% of assimilated dietary
376 MeHg is absorbed and mostly stored in muscle (Maury-Brachet et al., 2006), only 10% of iHg
377 remains in the organism (Gentès et al., 2015). For this reason, we usually find very low levels
378 of iHg (Wang and Wong, 2003). In the presence of a local point source of iHg, however, this
379 form can accumulate at higher rates in both liver and muscle tissue (Feng et al., 2015).

380 The majority of Hg accumulated in BS liver is in an inorganic form ($\approx 90\%$, Figure 3). Thus,
381 the near-zero $\Delta^{199}\text{Hg}$ values presented by BS seabass liver could reflect the isotopic
382 composition of iHg accumulated directly from the environment (Figure 3b). On the other
383 hand, BS muscle presents both Hg species, with a majority of MeHg (60-90%). In that case,
384 $\Delta^{199}\text{Hg}$ values in this tissue could represent a mix of multiple sources. $\Delta^{199}\text{Hg}$ values around
385 1.5‰ could represent MeHg coming from the diet, whilst lower MIF could be linked to the
386 remaining 10-40% of iHg. This is confirmed by the positive correlation between $\Delta^{199}\text{Hg}$
387 values and %MeHg in muscle (Figure 3b).

388 Inorganic Hg coming from industrial sources can have near-zero $\Delta^{199}\text{Hg}$, while watershed
389 loading can even impart negative MIF (Du et al., 2018; Lepak et al., 2015). Therefore, one

390 possibility for the low hepatic MIF might be that Hg stored in BS seabass liver comes from a
391 local point source of industrial origin (Wiederhold et al., 2015). The BS samples were taken
392 along the northern Turkish coast, between the Sinop peninsula and the Kızılırmak estuary.
393 This area is known for heavy industrial activity and the input of totally unregulated and
394 uncontrolled drainage water from upriver mining and agricultural areas (Bat et al., 2010;
395 Gökkurt et al., 2007). However, recent literature has shown that the amount of freshwater
396 discharge of particulate Hg in this locality, and its bioaccumulation in marine biota, is
397 negligible compared to other trace elements (e.g. $< 50 \text{ ng.g}^{-1}$ ww in fish liver, $< \text{DL}$ in
398 invertebrates) (Bat et al., 2019, 2018). Therefore, our Black Sea sampling site can be
399 considered as a relatively unpolluted area with regards to Hg (Table 1), excluding the
400 hypothesis of a particular point source of anthropogenic origin. Additionally, in Figure 1b we
401 can see how the values of the $\Delta^{199}\text{Hg}/\Delta^{201}\text{Hg}$ slopes for both liver (1.69 ± 0.03) and muscle
402 (1.26 ± 0.02) confirm that all Hg accumulated in BS seabass derives from photo-demethylated
403 MeHg in the water column, in the same way as the other regions. This combination of
404 evidence excludes our hypothesis of the presence of an additional source of iHg in the Black
405 Sea population.

406
407 **$\Delta^{199}\text{Hg}$ MIF of uncontaminated Black Sea waters show short-term ontogenetic shifts in**
408 **fish.**

409 Because of their different metabolic roles, muscle and liver tissues integrate different
410 time periods of the fish life cycle, and therefore also their habitat use and Hg exposure levels
411 (Madigan et al., 2012). One of the biggest complications in the interpretation of these kinds of
412 results is that isotopic and elemental uptake and excretion can occur at very different rates
413 (Carter et al., 2019). To our knowledge, there is no information about isotopic routing in fish
414 liver yet. However, if we consider that this is an organism where dietary MeHg is quickly

415 metabolized and accumulated as inert iHg with time, it is safe to accept that, as for mammals
416 and birds, it might integrate the entire life of the fish. MeHg half-life in fish muscle is much
417 shorter, around two years (Kwon et al., 2016; Tollefson and Cordle, 1986). Therefore, we
418 could propose that liver of BS seabass integrates information about Hg exposure during the
419 entire life of the fish, while muscle does so only for the last year. If this were the case, we
420 could hypothesize that the large MDF and MIF offsets between muscle and liver are showing
421 two separated temporal snapshots of the first year of life of BS seabass.

422 The seabass is a benthic-pelagic species which undergoes seasonal migrations between
423 their feeding (offshore) and spawning (estuaries) areas (Pawson et al., 1987). From birth until
424 their first year, immature fish inhabit their nursery areas (e.g. lagoons, estuaries) (López et al.,
425 2015). In some regions juvenile seabass can already start exploring offshore waters during
426 their first summer, but they never venture into deeper waters until they reach sexual maturity
427 (around five years of age) (Jennings et al., 1991).

428 Hepatic near-zero MIF and negative MDF of BS fish denote a coastal and benthic
429 habitat use, in accordance with previous literature about the trophic ecology of estuarine fish
430 (Kwon et al., 2014b; Li et al., 2016; Senn et al., 2010). In these areas, most Hg accumulated
431 in fish derives from MeHg formed in sediments (Li et al., 2016). The low MDF and MIF
432 values are a consequence of the reduced amount of photochemical degradation due to the
433 presence of more suspended particle loads and DOC concentrations that reduce light
434 penetration (Kwon et al., 2014b).

435 On the other hand, in marine offshore and pelagic food webs, MeHg derives mostly
436 from wet precipitation ($\Delta^{199}\text{Hg} = -1$ to 1‰) or deposition of gaseous elemental Hg ($\Delta^{199}\text{Hg} =$
437 0.5‰ to 1‰) (Kwon et al., 2020). This results in the high MIF values found in BS seabass
438 muscle (Figure 3b). Therefore, our findings suggest that in BS seabass, hepatic MIF, mostly
439 related to the iHg fraction, would represent the period of their life spent in the estuaries

440 feeding upon benthic invertebrates in the sediments. On the other hand, muscle—and the
441 isotopic composition related to MeHg—might show a more recent signature, corresponding to
442 the first exploratory trips to pelagic waters.

443 Cransveld *et al.* (2017) have thoroughly discussed the impact of seabass diet on MeHg
444 accumulation and Hg MDF and MIF values, integrating fish stomach content analysis with
445 the measurement of nitrogen and carbon stable isotope ratios ($\delta^{15}\text{N}$ and $\delta^{13}\text{C}$, respectively).

446 Although they found a difference in fish trophic level (TL, calculated from $\delta^{15}\text{N}$ values) and
447 $\delta^{13}\text{C}$ values, they did not find any correlation with seabass THg or MeHg concentrations
448 (Cransveld *et al.*, 2017). Stomach content revealed a similar variety of prey across all sites,
449 confirming the largely opportunistic feeding behavior of seabass (Cransveld *et al.*, 2017). This
450 further confirms that the differences in inter-organ MDF and MIF in BS fish, as well as the
451 other sites, depend more on shifts in habitat use than on diet.

452 Finally, while the very low contamination levels of the BS site allow the net differentiation of
453 local seabass from the other regions with regards to inter-tissue fractionation, it also separates
454 this subpopulation for the large heterogeneity of muscle MDF and MIF values (Figure 2).
455 This is linked with the unique oceanographic features of the Black Sea (e.g. low salinity,
456 strong freshwater input, semi-permanent stratification, etc.) (Bakan and Büyükgüngör, 2000;
457 Capet *et al.*, 2016; Özsoy and Ünlüata, 1997). These features lengthen marine Hg processing
458 and recycling between water layers, resulting in higher and more diverse $\Delta^{199}\text{Hg}$ and $\delta^{202}\text{Hg}$
459 values (Blum *et al.*, 2013; Motta *et al.*, 2019).

460 Our findings underline the necessity of collecting detailed information about the history of Hg
461 pollution, and its cycling and sourcing in the environment, before studying its accumulation,
462 organotropism and transformation within marine predatory fish through the analysis of Hg
463 stable isotope ratios.

464

465 **Conclusion**

466 The main findings of this study can be summarized as follows:

- 467 1. The multi-tissue comparison of Hg MDF and MIF signals produced evidence of
468 MeHg demethylation in the liver of a fish species, as well as trace Hg accumulation
469 dynamics between different populations of a marine predator;
- 470 2. In general, the levels of environmental Hg pollution influence Hg organotropism and
471 apparently also the extent of hepatic demethylation in marine predatory fish. However,
472 it is not the only factor contributing to Hg isotopic variability in the European seabass;
- 473 3. In highly contaminated areas, inter-organ MDF might get hindered by Hg saturation in
474 fish tissues. This has to be taken into account in the interpretation of Hg stable
475 isotopes in further studies. On the other hand, in uncontaminated sites ($< 200 \text{ ng.g}^{-1}$
476 dw in fish) such as the Black Sea, the inter-organ Hg MDF and MIF can trace short-
477 term shifts in fish habitat use;
- 478 4. Additionally, the particular oceanographic features of the Black Sea basin influence
479 Hg cycling and processing in the water column, as highlighted by BS seabass $\Delta^{199}\text{Hg}$
480 and $\delta^{202}\text{Hg}$ values.

481

482 **Acknowledgments**

483 Alice Cransveld and Marianna Pinzone acknowledge a PhD F.R.I.A. grant (F.R.S-FNRS).
484 Krishna Das is a Senior F.R.S.-FNRS Research Associate (Fond pour la Recherche
485 Scientifique). The authors thank Emmanuil Koutrakis (Fisheries Research Institute, Hellenic
486 Agricultural Organisation, Greece), Ayaka Ozturk (Faculty of Fisheries, Istanbul University,
487 Turkey), Nicola Bettoso (Agenzia Regionale per la Protezione dell'Ambiente del Friuli
488 Venezia Giulia [ARPA FVG], Italy) and Cláudia Mieiro (CESAM and Departamento de
489 Biologia, Universidade de Aveiro, Portugal) for their help in sampling the seabass. The

490 authors thank the members of the LCABIE, and the IPREM institute from Pau University for
 491 their warm welcome and for sharing their knowledge and expertise with us. Special thanks to
 492 Julien Barre for his constant help and guidance in the laboratory, and to Caiyan Feng for her
 493 practical assistance in some GC-ICP-MS analysis. English proofing was conducted by the
 494 Skylark Academic & Book Editing service (Invoice N° 427). The authors would like to pay
 495 tribute to the memory of the late Mr. Renzo Biondo for his support in laboratory analyses.

496

497 References

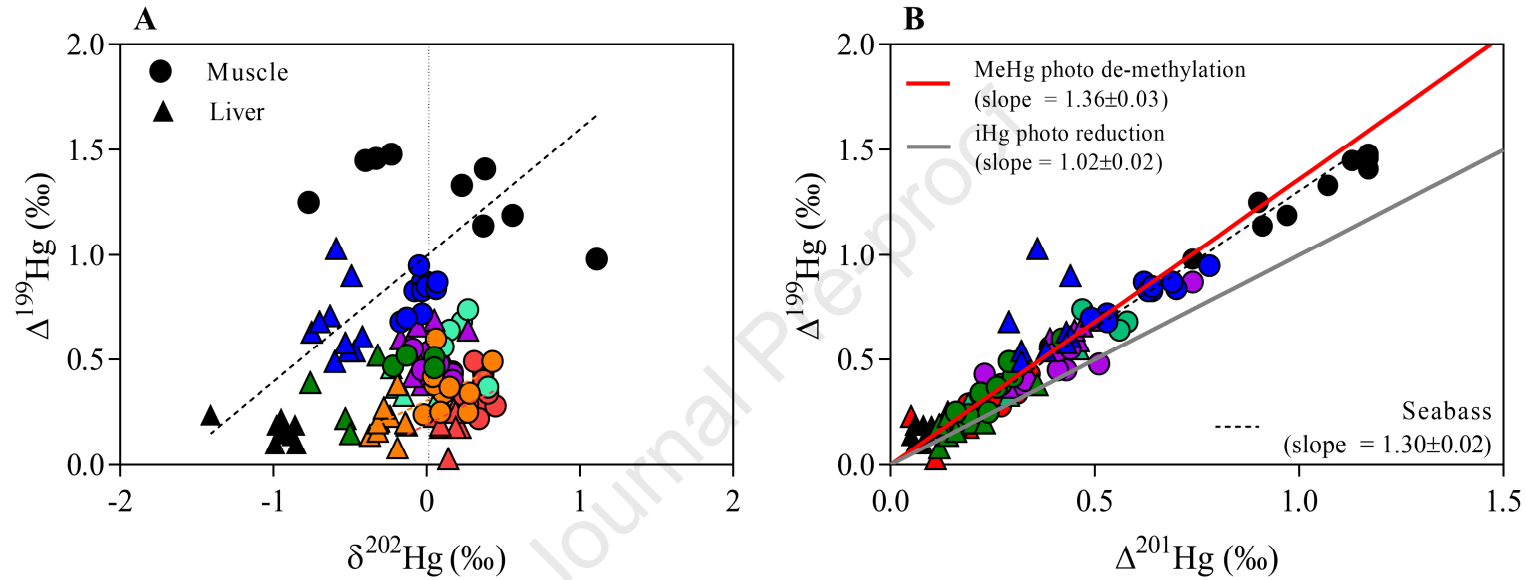
- 498 Bakan, G., Büyükgüngör, H., 2000. The Black Sea. *Mar. Pollut. Bull.* 41, 24–43. doi:10.1016/S0025-
 499 326X(00)00100-4
- 500 Bat, L., Gökkurt, O., Sezgin, M., Üstün, F., Sahin, F., 2010. Evaluation of the Black Sea Land Based Sources of
 501 Pollution the Coastal Region of Turkey. *Open Mar. Biol. J.* 3, 112–124.
 502 doi:10.2174/1874450800903010112
- 503 Bat, L., Şahin, F., Öztekin, A., 2019. Metal Bioaccumulation of *Mytilaster lineatus* (Gmelin, 1791) Collected
 504 From Sinop Coast in the Southern Black Sea. *Eur. J. Biol.* 78, 23–28. doi:10.26650/eurjbiol.2019.0001
- 505 Bat, L., Sezgin, M., Sahin, F., 2018. Heavy metal contamination of aquatic resources from Turkish Black Sea
 506 waters. *J. Environ. Prot. Ecol.* 19, 558–563.
- 507 Bergquist, B.A., Blum, J.D., 2009. The odds and evens of mercury isotopes: Applications of mass-dependent
 508 and mass-independent isotope fractionation. *Elements* 5, 353–357. doi:10.2113/gselements.5.6.353
- 509 Bergquist, B.A., Blum, J.D., 2007. Mass-dependent and -independent fractionation of hg isotopes by
 510 photoreduction in aquatic systems. *Science (80-.)*. 318, 417–420. doi:10.1126/science.1148050
- 511 Blum, J.D., Popp, B.N., Drazen, J.C., Anela Choy, C., Johnson, M.W., 2013. Methylmercury production below
 512 the mixed layer in the North Pacific Ocean. *Nat. Geosci.* 6, 879–884. doi:10.1038/ngeo1918
- 513 Blum, J.D., Sherman, L.S., Johnson, M.W., 2014. Mercury Isotopes in Earth and Environmental Sciences. *Annu.*
 514 *Rev. Earth Planet. Sci.* 42, 249–269. doi:10.1146/annurev-earth-050212-124107
- 515 Booth, S., Zeller, D., 2005. Mercury, food webs, and marine mammals: implications of diet and climate change
 516 for human health. *Environ. Health Perspect.* 113, 521–526.
- 517 Bystrom, E., 2008. Assessment of Mercury Methylation and Demethylation with Focus on Chemical Speciation
 518 and Biological Processes. Georgia Institute of Technology.
- 519 Capet, A., Stanev, E. V., Beckers, J.M., Murray, J.W., Grégoire, M., 2016. Decline of the Black Sea oxygen
 520 inventory. *Biogeosciences* 13, 1287–1297. doi:10.5194/bg-13-1287-2016
- 521 Carter, W.A., Bauchinger, U., McWilliams, S.R., 2019. The importance of isotopic turnover for understanding
 522 key aspects of animal ecology and nutrition. *Diversity* 11. doi:10.3390/D11050084
- 523 Chandan, P., Ghosh, S., Bergquist, B.A., 2015. Mercury Isotope Fractionation during Aqueous Photoreduction
 524 of Monomethylmercury in the Presence of Dissolved Organic Matter. *Environ. Sci. Technol.* 49, 259–267.
 525 doi:10.1021/es5034553
- 526 Christophoridis, A., Stamatis, N., Orfanidis, S., 2007. Sediment heavy metals of a mediterranean coastal lagoon:
 527 Agiasma, nestos delta, eastern macedonia (greece). *Transitional Waters Bull.* 1, 33–43.
 528 doi:10.1285/i1825229Xv1n4p33
- 529 Cizdziel, J., Hinnert, T., Cross, C., Pollard, J., 2003. Distribution of mercury in the tissues of five species of
 530 freshwater fish from Lake Mead, USA. *J. Environ. Monit.* 5, 802–807. doi:10.1039/b307641p
- 531 Coelho, J.P., Pereira, M.E., Duarte, A., Pardal, M.A., 2005. Macroalgae response to a mercury contamination
 532 gradient in a temperate coastal lagoon (Ria de Aveiro, Portugal). *Estuar. Coast. Shelf Sci.* 65, 492–500.
 533 doi:10.1016/j.ecss.2005.06.020
- 534 Cransveld, A., Amouroux, D., Tessier, E., Koutrakis, E., Ozturk, A.A., Bettoso, N., Mieiro, C.L., Bérail, S.,
 535 Barre, J.P.G., Sturaro, N., Schnitzler, J., Das, K., 2017. Mercury Stable Isotopes Discriminate Different
 536 Populations of European Seabass and Trace Potential Hg Sources around Europe. *Environ. Sci. Technol.*
 537 51, 12219–12228. doi:10.1021/acs.est.7b01307
- 538 Du, B., Feng, X., Li, P., Yin, R., Yu, B., Sonke, J.E., Guinot, B., Anderson, C.W.N., Maurice, L., 2018. Use of

- 539 Mercury Isotopes to Quantify Mercury Exposure Sources in Inland Populations, China. *Environ. Sci.*
540 *Technol.* 52, 5407–5416. doi:10.1021/acs.est.7b05638
- 541 Du, H., Ma, M., Igarashi, Y., Wang, D., 2019. Biotic and Abiotic Degradation of Methylmercury in Aquatic
542 Ecosystems: A Review. *Bull. Environ. Contam. Toxicol.* 102, 605–611. doi:10.1007/s00128-018-2530-2
- 543 Eagles-Smith, C.A., Ackerman, J.T., Yee, J., Adelsbach, T.L., 2009. Mercury demethylation in waterbird livers:
544 dose-response thresholds and differences among species. *Environ. Toxicol. Chem.* 28, 568–77.
545 doi:10.1897/08-245.1
- 546 Feng, C., Pedrero, Z., Gentès, S., Barre, J., Renedo, M., Tessier, E., Berail, S., Maury-Brachet, R., Mesmer-
547 Dudons, N., Baudrimont, M., Legeay, A., Maurice, L., Gonzalez, P., Amouroux, D., 2015. Specific
548 Pathways of Dietary Methylmercury and Inorganic Mercury Determined by Mercury Speciation and
549 Isotopic Composition in Zebrafish (*Danio rerio*). *Environ. Sci. Technol.* 49, 12984–12993.
550 doi:10.1021/acs.est.5b03587
- 551 Foucher, D., Ogrinc, H., Hintelmann, H., 2009. Tracing Mercury Contamination from the Idrija Mining Region
552 (Slovenia) to the Gulf of Trieste Using Hg Isotope Ratio Measurements. *Environ. Sci. Technol.* 43, 33–39.
553 doi:10.1021/es801772b
- 554 Gantner, N., Hintelmann, H., Zheng, W., Muir, D.C., 2009. Variations in stable isotope fractionation of Hg in
555 food webs of Arctic lakes. *Environ. Sci. Technol.* 43, 9148–9154. doi:10.1021/es901771r
- 556 Gehrke, G.E., Blum, J.D., Slotton, D.G., Greenfield, B.K., 2011. Mercury Isotopes Link Mercury in San
557 Francisco Bay Forage Fish to Surface Sediments. *Environ. Sci. Technol.* 45, 1264–1270.
558 doi:10.1021/es103053y
- 559 Gentès, S., Maury-Brachet, R., Feng, C., Pedrero, Z., Tessier, E., Legeay, A., Mesmer-Dudons, N., Baudrimont,
560 M., Maurice, L., Amouroux, D., Gonzalez, P., 2015. Specific Effects of Dietary Methylmercury and
561 Inorganic Mercury in Zebrafish (*Danio rerio*) Determined by Genetic, Histological, and Metallothionein
562 Responses. *Environ. Sci. Technol.* 49, 14560–14569. doi:10.1021/acs.est.5b03586
- 563 Gökkurt, O., Bat, L., Sahin, F., 2007. The investigation of some physicochemical parameters in the Middle
564 Black Sea (Sinop, Turkey)., in: *Proceedings of 7th National Environmental Engineering Congress*. pp.
565 869–873.
- 566 Gonzalez, P., Dominique, Y., Massabuau, J.C., Boudou, A., Bourdineaud, J.P., 2005. Comparative Effects of
567 Dietary Methylmercury on Gene Expression in Liver, Skeletal Muscle, and Brain of the Zebrafish (*Danio*
568 *rerio*). *Environ. Sci. Technol.* 39, 3972–3980. doi:10.1021/es0483490
- 569 Gratz, L.E., Keeler, G.J., Blum, J.D., Sherman, L.S., 2010. Isotopic composition and fractionation of mercury in
570 Great Lakes precipitation and ambient air. *Environ. Sci. Technol.* 44, 7764–7770. doi:10.1021/es100383w
- 571 Guilherme, S., Válega, M., Pereira, M.E., Santos, M.A., Pacheco, M., 2008. Antioxidant and biotransformation
572 responses in *Liza aurata* under environmental mercury exposure - Relationship with mercury accumulation
573 and implications for public health. *Mar. Pollut. Bull.* 56, 845–859. doi:10.1016/j.marpolbul.2008.02.003
- 574 Gworek, B., Bemowska-Kałabun, O., Kijeńska, M., Wrzosek-Jakubowska, J., 2016. Mercury in Marine and
575 Oceanic Waters—a Review. *Water. Air. Soil Pollut.* 227. doi:10.1007/s11270-016-3060-3
- 576 Habran, S., Crocker, D.E., Debier, C., Das, K., 2012. How are trace elements mobilized during the postweaning
577 fast in Northern elephant seals? *Environ. Toxicol. Chem.* 31, 2354–2365. doi:10.1002/etc.1960
- 578 Havelková, M., Dušek, L., Némethová, D., Poleszczuk, G., Svobodová, Z., 2008. Comparison of mercury
579 distribution between liver and muscle - A biomonitoring of fish from lightly and heavily contaminated
580 localities. *Sensors* 8, 4095–4109. doi:10.3390/s8074095
- 581 Hong, Y.-S., Kim, Y.-M., Lee, K.-E., 2012. Methylmercury exposure and health effects. *J. Prev. Med. public*
582 *Heal.* 45, 353–363. doi:10.3961/jpmph.2012.45.6.353
- 583 Jardine, T., Kidd, K.A., Fisk, A.T., 2006. Critical Review Applications, Considerations, and Sources of
584 Uncertainty When Using Stable Isotope Analysis in Ecotoxicology. *Crit. Rev.* 40, 7501–7511.
585 doi:10.1021/es061263h
- 586 Jennings, S., Lancaster, J.E., Ryland, J.S., Shackley, S.E., 1991. The age structure and growth dynamics of
587 young-of-the-year bass, *dicentrarchus labrax*, populations. *J. Mar. Biol. Assoc. United Kingdom* 71, 799–
588 810. doi:10.1017/S0025315400053467
- 589 Kritee, K., Motta, L.C., Blum, J.D., Tsui, M.T.K., Reinfelder, J.R., 2018. Photomicrobial Visible Light-Induced
590 Magnetic Mass Independent Fractionation of Mercury in a Marine Microalga. *ACS Earth Sp. Chem.* 2,
591 432–440. doi:10.1021/acsearthspacechem.7b00056
- 592 Kwon, S.Y., Blum, J.D., Carvan, M.J., Basu, N., Head, J.A., Madenjian, C.P., David, S.R., 2012. Absence of
593 Fractionation of Mercury Isotopes during Trophic Transfer of Methylmercury to Freshwater Fish in
594 Captivity. *Environ. Sci. Technol.* 46, 7527–7534. doi:10.1021/es300794q
- 595 Kwon, S.Y., Blum, J.D., Chen, C.Y., Meattay, D.E., Mason, R.P., 2014a. Mercury Isotope Study of Sources and
596 Exposure Pathways of Methylmercury in Estuarine Food Webs in the Northeastern U.S. *Environ. Sci.*
597 *Technol.* 48, 10089–10097. doi:10.1021/es5020554
- 598 Kwon, S.Y., Blum, J.D., Chen, C.Y., Meattay, D.E., Mason, R.P., 2014b. Mercury isotope study of sources and

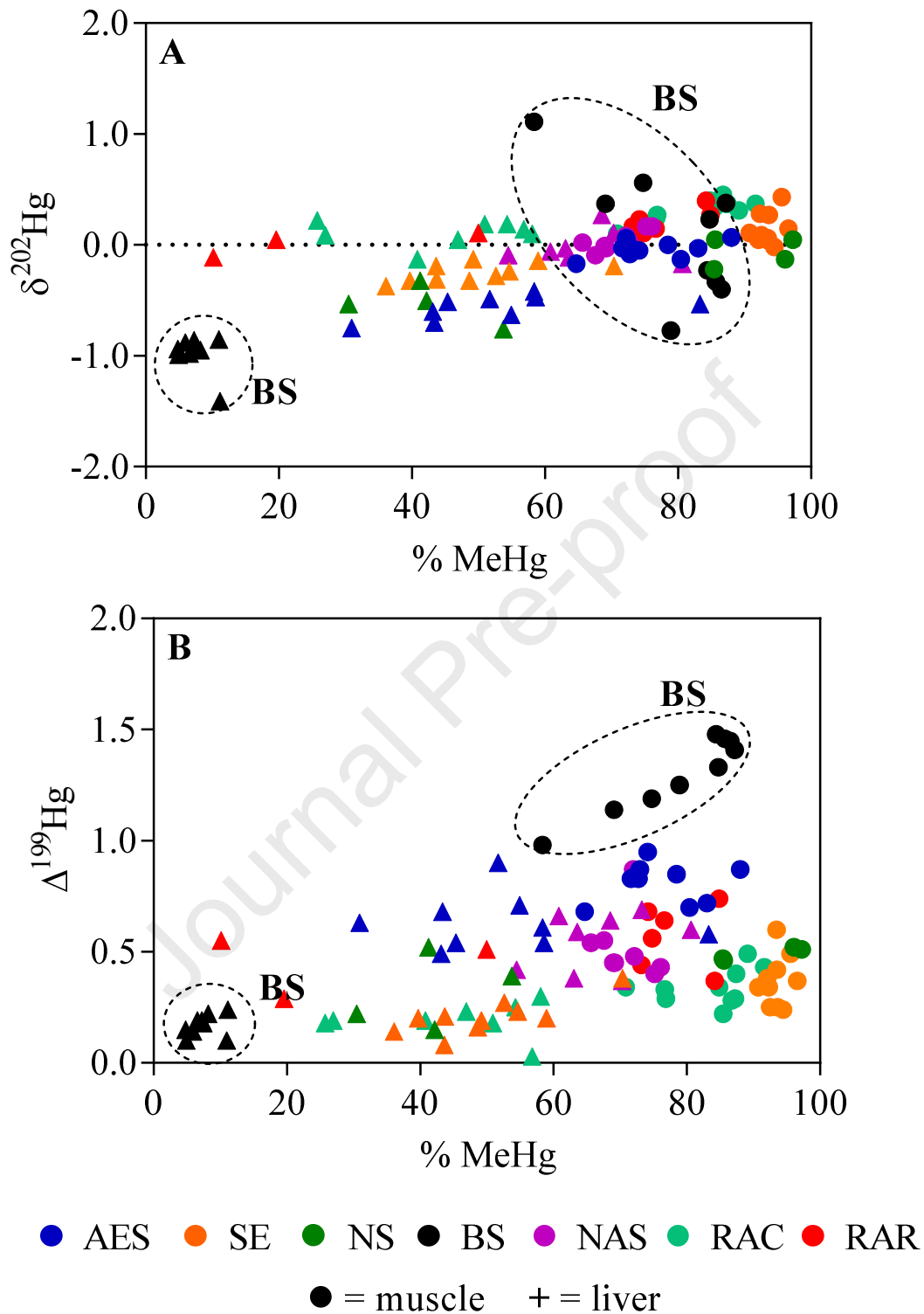
- 599 exposure pathways of methylmercury in estuarine food webs in the northeastern U.S. *Environ. Sci.*
 600 *Technol.* 48, 10089–10097. doi:10.1021/es5020554
- 601 Kwon, S.Y., Blum, J.D., Madigan, D.J., Block, B.A., Popp, B.N., 2016. Quantifying mercury isotope dynamics
 602 in captive Pacific bluefin tuna (*Thunnus orientalis*). *Elem. Sci. Anthr.* 4, 000088.
 603 doi:10.12952/journal.elementa.000088
- 604 Kwon, S.Y., Blum, J.D., Yin, R., Tsui, M.T.K., Yang, Y.H., Choi, J.W., 2020. Mercury stable isotopes for
 605 monitoring the effectiveness of the Minamata Convention on Mercury. *Earth-Science Rev.* 203, 103111.
 606 doi:10.1016/j.earscirev.2020.103111
- 607 Lang, T., Kruse, R., Haarich, M., Wosniok, W., 2017. Mercury species in dab (*Limanda limanda*) from the
 608 North Sea, Baltic Sea and Icelandic waters in relation to host-specific variables. *Mar. Environ. Res.* 124,
 609 32–40. doi:10.1016/j.marenvres.2016.03.001
- 610 Le Croizier, G., Lorrain, A., Sonke, J.E., Jaquemet, S., Schaal, G., Renedo, M., Besnard, L., Cherel, Y., Point,
 611 D., 2020. Mercury isotopes as tracers of ecology and metabolism in two sympatric shark species. *Environ.*
 612 *Pollut.* 265. doi:10.1016/j.envpol.2020.114931
- 613 Lehnherr, I., St. Louis, V.L., 2009. Importance of ultraviolet radiation in the photodemethylation of
 614 methylmercury in freshwater ecosystems. *Environ. Sci. Technol.* 43, 5692–5698. doi:10.1021/es9002923
- 615 Lepak, R.F., Yin, R., Krabbenhoft, D.P., Ogorek, J.M., Dewild, J.F., Holsen, T.M., Hurley, J.P., 2015. Use of
 616 Stable Isotope Signatures to Determine Mercury Sources in the Great Lakes. *Environ. Sci. Technol. Lett.*
 617 2, 335–341. doi:10.1021/acs.estlett.5b00277
- 618 Li, M., Juang, C.A., Ewald, J.D., Yin, R., Mikkelsen, B., Krabbenhoft, D.P., Balcom, P.H., Dassuncao, C.,
 619 Sunderland, E.M., 2020. Selenium and stable mercury isotopes provide new insights into mercury
 620 toxicokinetics in pilot whales. *Sci. Total Environ.* 710, 136325. doi:10.1016/j.scitotenv.2019.136325
- 621 Li, M., Schartup, A.T., Valberg, A.P., Ewald, J.D., Krabbenhoft, D.P., Yin, R., Balcom, P.H., Sunderland, E.M.,
 622 2016. Environmental Origins of Methylmercury Accumulated in Subarctic Estuarine Fish Indicated by
 623 Mercury Stable Isotopes. *Environ. Sci. Technol.* 50, 11559–11568. doi:10.1021/acs.est.6b03206
- 624 López, R., De Pontual, H., Bertignac, M., Mahévas, S., 2015. What can exploratory modelling tell us about the
 625 ecobiology of European sea bass (*Dicentrarchus labrax*): A comprehensive overview. *Aquat. Living*
 626 *Resour.* 28, 61–79. doi:10.1051/alr/2015007
- 627 Lu, X., Liu, Y., Johs, A., Zhao, L., Wang, T., Yang, Z., Lin, H., Elias, D.A., Pierce, E.M., Liang, L., Barkay, T.,
 628 Gu, B., 2016. Anaerobic Mercury Methylation and Demethylation by *Geobacter bemidjiensis* Bem.
 629 *Environ. Sci. Technol.* 50, 4366–4373. doi:10.1021/acs.est.6b00401
- 630 Luo, H., Cheng, Q., Pan, X., 2020. Photochemical behaviors of mercury (Hg) species in aquatic systems: A
 631 systematic review on reaction process, mechanism, and influencing factor. *Sci. Total Environ.* 720,
 632 137540. doi:10.1016/j.scitotenv.2020.137540
- 633 Madigan, D.J., Litvin, S.Y., Popp, B.N., Carlisle, A.B., Farwell, C.J., Block, B.A., 2012. Tissue Turnover Rates
 634 and Isotopic Trophic Discrimination Factors in the Endothermic Teleost, Pacific Bluefin Tuna (*Thunnus*
 635 *orientalis*). *PLoS One* 7. doi:10.1371/journal.pone.0049220
- 636 Man, Y., Yin, R., Cai, K., Qin, C., Wang, J., Yan, H., Li, M., 2019. Primary amino acids affect the distribution
 637 of methylmercury rather than inorganic mercury among tissues of two farmed-raised fish species.
 638 *Chemosphere* 225, 320–328. doi:10.1016/j.chemosphere.2019.03.058
- 639 Mason, R.P., Lawson, N.M., Sheu, G.R., 2001. Mercury in the atlantic ocean: Factors controlling air-sea
 640 exchange of mercury and its distribution in the upper waters. *Deep. Res. Part II Top. Stud. Oceanogr.* 48,
 641 2829–2853. doi:10.1016/S0967-0645(01)00020-0
- 642 Maury-Brachet, R., Durrieu, G., Dominique, Y., Boudou, A., 2006. Mercury distribution in fish organs and food
 643 regimes: Significant relationships from twelve species collected in French Guiana (Amazonian basin). *Sci.*
 644 *Total Environ.* 368, 262–270. doi:http://dx.doi.org/10.1016/j.scitotenv.2005.09.077
- 645 Mieiro, C., Pacheco, M., Pereira, M., Duarte, A., 2011. Mercury Organotropism in Feral European Sea Bass
 646 (*Dicentrarchus labrax*). *Arch. Environ. Contam. Toxicol.* 61, 135–143. doi:10.1007/s00244-010-9591-5
- 647 Mieiro, C.L., Pacheco, M., Pereira, M.E., Duarte, A.C., 2009. Mercury distribution in key tissues of fish (*Liza*
 648 *aurata*) inhabiting a contaminated estuary - Implications for human and ecosystem health risk assessment.
 649 *J. Environ. Monit.* 11, 1004–1012. doi:10.1039/b821253h
- 650 Motta, L.C., Blum, J.D., Johnson, M.W., Umhau, B.P., Popp, B.N., Washburn, S.J., Drazen, J.C., Benitez-
 651 Nelson, C.R., Hannides, C.C.S., Close, H.G., Lamborg, C.H., 2019. Mercury Cycling in the North Pacific
 652 Subtropical Gyre as Revealed by Mercury Stable Isotope Ratios. *Global Biogeochem. Cycles* 33, 777–794.
 653 doi:10.1029/2018GB006057
- 654 Mozaffarian, D., Rimm, E.B., 2008. Fish intake, contaminants, and human health evaluating the risks and the
 655 benefits. *J. Am. Med. Assoc.* 296, 1885–1899.
- 656 Obrist, D., Kirk, J.L., Zhang, L., Sunderland, E.M., Jiskra, M., Selin, N.E., 2018. A review of global
 657 environmental mercury processes in response to human and natural perturbations: Changes of emissions,
 658 climate, and land use. *Ambio* 47, 116–140. doi:10.1007/s13280-017-1004-9

- 659 Oliveira Ribeiro, C.A., Rouleau, C., Pelletier, É., Audet, C., Tjälve, H., 1999. Distribution Kinetics of Dietary
660 Methylmercury in the Arctic Charr (*Salvelinus alpinus*). *Environ. Sci. Technol.* 33, 902–907.
661 doi:10.1021/es980242n
- 662 Özsoy, E., Ünlüata, Ü., 1997. Oceanography of the Black Sea: A review of some recent results. *Earth-Science*
663 *Rev.* 42, 231–272. doi:10.1016/S0012-8252(97)81859-4
- 664 Pawson, M.G., Pickett, G.D., Kelley, D.F., 1987. The distribution and migrations of bass, *Dicentrarchus labrax*
665 L., in waters around England and Wales as shown by tagging. *J. Mar. Biol. Assoc. United Kingdom* 67,
666 183–217. doi:https://doi.org/10.1017/S0025315400026448
- 667 Pentreath, R.J., 1976. The accumulation of mercury from food by the plaice, *Pleuronectes platessa* L. *J.*
668 *Exp. Mar. Bio. Ecol.* 25, 51–65.
- 669 Perga, M.E., Gerdeaux, D., 2005. `Are fish what they eat' all year round? *Oecologia* 144, 598–606.
670 doi:10.1007/s00442-005-0069-5
- 671 Perrot, V., Epov, V.N., Pastukhov, M. V., Grebenshchikova, V.I., Zouiten, C., Sonke, J.E., Husted, S., Donard,
672 O.F.X., Amouroux, D., 2010. Tracing Sources and Bioaccumulation of Mercury in Fish of Lake Baikal–
673 Angara River Using Hg Isotopic Composition. *Environ. Sci. Technol.* 44, 8030–8037.
674 doi:10.1021/es101898e
- 675 Perrot, V., Masbou, J., Pastukhov, M. V., Epov, V.N., Point, D., Bérail, S., Becker, P.R., Sonke, J.E.,
676 Amouroux, D., 2015. Natural Hg isotopic composition of different Hg compounds in mammal tissues as a
677 proxy for in vivo breakdown of toxic methylmercury. *Metallomics* 8, 170–178. doi:10.1039/c5mt00286a
- 678 Pinzone, M., Acquarone, M., Huyghebaert, L., Sturaro, N., Michel, L.N., Siebert, U., Das, K., 2017. Carbon,
679 nitrogen and sulphur isotopic fractionation in captive juvenile hooded seal (*Cystophora cristata*):
680 Application for diet analysis. *Rapid Commun. Mass Spectrom.* 31. doi:10.1002/rcm.7955
- 681 Point, D., Sonke, J.E., Day, R.D., Roseneau, D.G., Hobson, K.A., Pol, S.S. Vander, Moors, A.J., Pugh, R.S.,
682 Donard, O.F.X., Becker, P.R., 2011. Methylmercury photodegradation influenced by sea-ice cover in
683 Arctic marine ecosystems. *Nat. Geosci.* 4, 188–194. doi:10.1038/ngeo1049
- 684 Regnell, O., Watras, C.J., 2019. Microbial Mercury Methylation in Aquatic Environments: A Critical Review of
685 Published Field and Laboratory Studies. *Environ. Sci. Technol.* 53, 4–19. doi:10.1021/acs.est.8b02709
- 686 Renedo, M., Amouroux, D., Duval, B., Carravieri, A., Tessier, E., Barre, J., Bérail, S., Pedrero, Z., Cherel, Y.,
687 Bustamante, P., 2018. Seabird Tissues As Efficient Biomonitoring Tools for Hg Isotopic Investigations:
688 Implications of Using Blood and Feathers from Chicks and Adults. *Environ. Sci. Technol.* 52, 4227–4234.
689 doi:10.1021/acs.est.8b00422
- 690 Renedo, M., Pedrero, Z., Amouroux, D., Cherel, Y., Bustamante, P., 2021. Mercury isotopes of key tissues
691 document mercury metabolic processes in seabirds. *Chemosphere* 263, 127777.
692 doi:10.1016/j.chemosphere.2020.127777
- 693 Renzoni, A., Zino, F., Franchi, E., 1998. Mercury Levels along the Food Chain and Risk for Exposed
694 Populations. *Environ. Res.* 77, 68–72. doi:http://dx.doi.org/10.1006/enrs.1998.3832
- 695 Rodríguez Martín-Doimeadios, R.C., Krupp, E., Amouroux, D., Donard, O.F.X., 2002. Application of
696 Isotopically Labeled Methylmercury for Isotope Dilution Analysis of Biological Samples Using Gas
697 Chromatography/ICPMS. *Anal. Chem.* 74, 2505–2512. doi:10.1021/ac011157s
- 698 Rua-Ibarz, A., Bolea-Fernandez, E., Maage, A., Frantzen, S., Sanden, M., Vanhaecke, F., 2019. Tracing Mercury
699 Pollution along the Norwegian Coast via Elemental, Speciation, and Isotopic Analysis of Liver and Muscle
700 Tissue of Deep-Water Marine Fish (*Brosme brosme*). *Environ. Sci. Technol.* 53, 1776–1785.
701 doi:10.1021/acs.est.8b04706
- 702 Senn, D.B., Chesney, E.J., Blum, J.D., Bank, M.S., Maage, A., Shine, J.P., 2010. Stable isotope (N, C, Hg) study
703 of methylmercury sources and trophic transfer in the Northern Gulf of Mexico. *Environ. Sci. Technol.* 44,
704 1630–1637.
- 705 Serrell, N., Chen, C.Y., Lambert, K.F., Driscoll, C.T., Mason, R.P., Sunderland, E.M., Rardin, L.R., 2012.
706 Marine mercury fate: From sources to seafood consumers. *Environ. Res.* 119, 1–2.
707 doi:10.1016/j.envres.2012.10.001
- 708 Sherman, L.S., Blum, J.D., 2013. Mercury stable isotopes in sediments and largemouth bass from Florida lakes,
709 USA. *Sci. Total Environ.* 448, 163–175. doi:http://dx.doi.org/10.1016/j.scitotenv.2012.09.038
- 710 Sherman, L.S., Blum, J.D., Johnson, K.P., Keeler, G.J., Barres, J.A., Douglas, T.A., 2010. Mass-independent
711 fractionation of mercury isotopes in Arctic snow driven by sunlight. *Nat. Geosci.* 3, 173–177.
712 doi:10.1038/ngeo758
- 713 Sonke, J.E., Heimbürger, L.E., Dommergue, A., 2013. Mercury biogeochemistry: Paradigm shifts, outstanding
714 issues and research needs. *Comptes Rendus - Geosci.* 345, 213–224. doi:10.1016/j.crte.2013.05.002
- 715 Sonne, C., Aspholm, O., Dietz, R., Andersen, S., Berntssen, M.H.G., Hylland, K., 2009. A study of metal
716 concentrations and metallothionein binding capacity in liver, kidney and brain tissues of three Arctic seal
717 species. *Sci. Total Environ.* 407, 6166–6172. doi:10.1016/j.scitotenv.2009.08.029
- 718 Sunderland, E.M., Dalziel, J., Heyes, A., Branfireun, B.A., Krabbenhoft, D.P., Gobas, F.A.P.C., 2010. Response

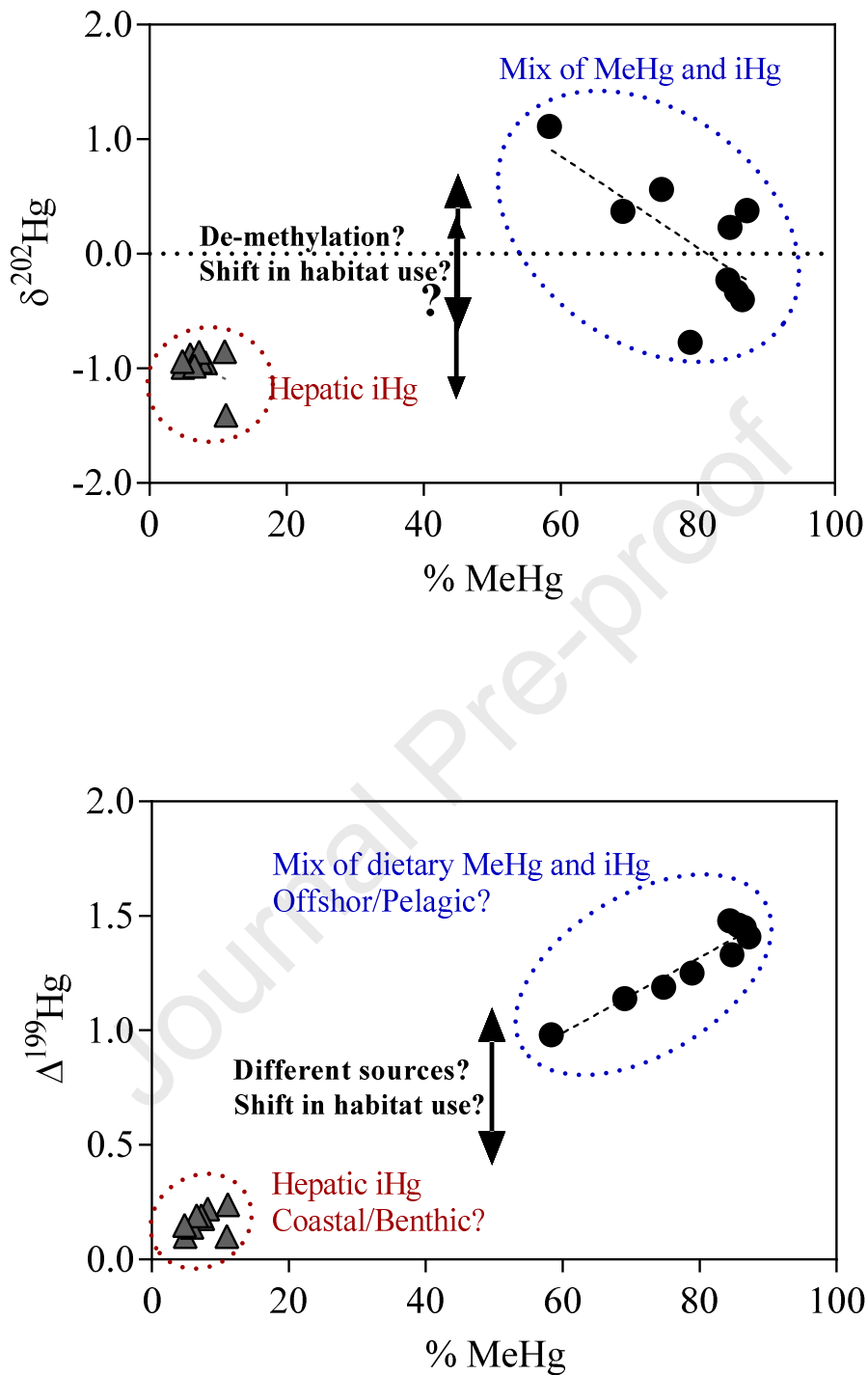
- 719 of a macrotidal estuary to changes in anthropogenic mercury loading between 1850 and 2000. *Environ.*
720 *Sci. Technol.* 44, 1698–1704. doi:10.1021/es9032524
- 721 Tollefson, L., Cordle, F., 1986. Methylmercury in fish: A review of residue levels, fish consumption and
722 regulatory action in the United States. *Environ. Health Perspect.* Vol. 68, 203–208.
723 doi:10.1289/ehp.8668203
- 724 Tsui, M.T.K., Blum, J.D., Kwon, S.Y., 2019. Review of stable mercury isotopes in ecology and
725 biogeochemistry. *Sci. Total Environ.* 135386. doi:10.1016/j.scitotenv.2019.135386
- 726 UNEP, 2018. Global Mercury Assessment 2018 270.
- 727 UNEP, 2013. Global Mercury Assessment 2013: Sources, emissions, releases and environmental transport.
728 United Nation Environment Programme Chemical Branch, Geneva, Switzerland.
- 729 Wagemann, R., Trebacz, E., Boila, G., Lockhart, W.L., 1998. Methylmercury and total mercury in tissues of
730 arctic marine mammals. *Sci. Total Environ.* 218, 19–31.
- 731 Wang, R., Feng, X. Bin, Wang, W.X., 2013. In vivo mercury methylation and demethylation in freshwater
732 tilapia quantified by mercury stable isotopes. *Environ. Sci. Technol.* 47, 7949–7957.
733 doi:10.1021/es3043774
- 734 Wang, W.X., Tan, Q.G., 2019. Applications of dynamic models in predicting the bioaccumulation, transport and
735 toxicity of trace metals in aquatic organisms. *Environ. Pollut.* 252, 1561–1573.
736 doi:10.1016/j.envpol.2019.06.043
- 737 Wang, W.X., Wong, R.S.K., 2003. Bioaccumulation kinetics and exposure pathways of inorganic mercury and
738 methylmercury in a marine fish, the sweetlips *Plectorhinchus gibbosus*. *Mar. Ecol. Prog. Ser.* 261, 257–
739 268.
- 740 Wang, X., Wu, F., Wang, W.X., 2017. In Vivo Mercury Demethylation in a Marine Fish (*Acanthopagrus*
741 *schlegeli*). *Environ. Sci. Technol.* 51, 6441–6451. doi:10.1021/acs.est.7b00923
- 742 Wiederhold, J.G., Skyllberg, U., Drott, A., Jiskra, M., Jonsson, S., Björn, E., Bourdon, B., Kretzschmar, R.,
743 2015. Mercury isotope signatures in contaminated sediments as a tracer for local industrial pollution
744 sources. *Environ. Sci. Technol.* 49, 177–185. doi:10.1021/es5044358
- 745 Yin, R., Feng, X., Hurley, J.P., Krabbenhoft, D.P., Lepak, R.F., Kang, S., Yang, H., Li, X., 2016. Historical
746 Records of Mercury Stable Isotopes in Sediments of Tibetan Lakes. *Sci. Rep.* 6, 23332.
747 doi:10.1038/srep23332
- 748 Zhang, T., Hsu-kim, H., 2010. Photolytic degradation of methylmercury enhanced by binding to natural organic
749 ligands. *Nat. Geosci.* 3, 473–476. doi:10.1038/ngeo892. Photolytic
- 750 Zheng, W., Hintelmann, H., 2009. Mercury isotope fractionation during photoreduction in natural water is
751 controlled by its Hg/DOC ratio. *Geochim. Cosmochim. Acta* 73, 6704–6715.
752 doi:10.1016/j.gca.2009.08.016
- 753 Živković, I., Kotnik, J., Šolić, M., Horvat, M., 2017. The abundance, distribution and speciation of mercury in
754 waters and sediments of the Adriatic sea - a review. *Acta Adriat.* 58, 165–186. doi:10.32582/aa.58.1.14
- 755
- 756

757 **Figures**

758
 759 **Figure 1.** MIF vs. MDF plot (A) and MIF vs. MIF plot (B) of muscle (circle) and liver (triangle) of European seabass (*D. labrax*) from AES
 760 (blue), NS (green), SE (orange), NAS (violet), BS (black), RAR (light green) and RAC (red). Significant correlation is shown by discontinuous
 761 regression lines.



762
 763 **Figure 2.** $\delta^{202}\text{Hg}$ (A) and $\Delta^{199}\text{Hg}$ (B) values vs. % MeHg for all sampling sites of muscle and
 764 liver tissue. AES = Aegean Sea (blue), NS = North Sea (Green), SE = Seine Estuary
 765 (Orange), BS = Black Sea (Black), NAS = North Adriatic Sea (NAS), RAR = Ria d'Aveiro
 766 Reference (Red) and RAC = Ria d'Aveiro Contaminated (Light blue). The dotted ellipse is a
 767 figurative grouping of BS seabass. Muscle values are represented by the circle, and liver
 768 values by the cross.



769
 770 **Figure 3.** $\delta^{202}\text{Hg}$ vs. MeHg (A) and $\Delta^{199}\text{Hg}$ vs. MeHg (B) in muscle (black dots) and liver
 771 (grey triangles) of the Black sea population of seabass *D. labrax*. MDF and MIF signatures
 772 are shown in per mill (‰), while MeHg proportion is represented in percentage (%).
 773 Significant correlation is represented by a discontinuous regression line.

774 **Tables**

775

776 **Table 1.** Summary of fish biometric information per sampling area. Information about local Hg sources at the sampling sites are extrapolated
 777 from literature and supporting information in Cransveld et al. (2017). Old pollution sources which are not active anymore are shown in italics.

Sampling Site	Standard length (cm)	Body mass (g)	Estimated age range (years)	Pollution sources	Definition*
AGEAN SEA AES	28 ± 1 (25 - 30) n= 10	272 ± 48 (205 - 380) n= 10	2	Protected by the Ramsar convention	Low Pollution
NORTH SEA NS	26 ± 6 (16 - 30) n= 10	192 ± 90 (43 - 278) n= 10	1 - 3	Interland industry Coastal urbanism	Moderate Pollution
SEINE ESTUARY SE	33 ± 2 (30 - 35) n= 10	487 ± 66 (350 - 563) n= 10	3 - 4	Interland industry Coastal urbanism	Moderate Pollution
BLACK SEA BS	21 ± 2 (18 - 24) n= 10	140 ± 24 (110 - 170) n= 10	1 - 2	Interland industry and agriculture	Low Pollution
NORTHERN ADRIATIC SEA NAS	22 ± 1 (20 - 23) n= 9	123 ± 20 (89 - 149) n= 9	1	<i>Idrija mercury mine</i> <i>Chlor-alkali plant</i> Coastal industry	High Pollution
RIA DE AVEIRO REFERENCE RAR	21 ± 4 (17 - 26) n= 10	106 ± 60 (55 - 217) n= 10	1 - 2	(Lagoon outlet) Coastal industry and urban development	Moderate Pollution
RIA DE AVEIRO CONTAMINATED RAC	17 ± 1 (16 - 18) n= 12	59 ± 10 (45 - 77) n= 12	1	(Laranjio Basin) <i>Chlor-alkali plant</i> Coastal industry and urban development	High Pollution

778 *We separated the sampling sites into three categories: "Low Pollution" for all the sites presenting THg = < 200ng.g⁻¹ dw, "Moderate Pollution" when THg ranged between
 779 500 and 1500 ng.g⁻¹ dw, and "High Pollution" when THg = >1500 ng.g⁻¹ dw, based on the statistical difference reported for muscle concentrations (*a*, *b* and *c* in Figure S1).

780

781
782
783
784

Table 2. THg and MeHg concentrations ($\text{ng}\cdot\text{g}^{-1}$, dw), %MeHg and Hg isotopic ratios (as δ and Δ values, ‰) in liver of *Dicentrarchus labrax* from seven sampling sites across Europe. All values are expressed as mean \pm standard deviation (SD), median (minimum-maximum) and n = number of analyzed samples.

SAMPLING SITE	[THg]	[MeHg]	%MeHg	$\delta^{202}\text{Hg}$	$\Delta^{199}\text{Hg}$	$\Delta^{200}\text{Hg}$	$\Delta^{201}\text{Hg}$	$\Delta^{204}\text{Hg}$
AGEAN SEA AES	166 \pm 37 182 (101 - 203) n= 10	89 \pm 34 86 (46 - 154) n= 9	52 \pm 15 52 (31 - 83) n= 9	-0.57 \pm 0.10 -0.56 (-0.75 - -0.42) n= 10	0.67 \pm 0.17 0.62 (0.49 - 1.03) n= 10	0.05 \pm 0.03 0.05 (0.00 - 0.09) n= 10	0.39 \pm 0.06 0.40 (0.29 - 0.49) n= 10	-0.12 \pm 0.08 -0.09 (-0.24 - -0.01) n= 10
NORTH SEA NS	840 \pm 575 827 (208 - 1498) n= 4	326 \pm 179 375 (86 -457) n= 4	42 \pm 10 42 (30 - 54) n= 4	-0.53 \pm 0.18 -0.51 (-0.76 - -0.32) n= 4	0.32 \pm 0.16 0.31 (0.15 - 0.52) n= 4	0.02 \pm 0.03 0.02 (-0.01 - 0.06) n= 4	0.12 \pm 0.07 0.15 (0.03 - 0.17) n= 4	-0.03 \pm 0.04 -0.02 (-0.08 - 0.02) n= 4
SEINE ESTUARY SE	1031 \pm 153 1016 (769 - 1228) n=10	512 \pm 111 536 (277 - 646) n= 10	50 \pm 10 49 (36 - 70) n= 10	-0.25 \pm 0.08 -0.26 (-0.37 - -0.13) n= 10	0.21 \pm 0.08 0.20 (0.08 - 0.38) n= 10	0.001 \pm 0.03 0.00 (-0.05 - 0.05) n= 10	0.19 \pm 0.07 0.17 (0.12 - 0.36) n= 10	0.01 \pm 0.06 -0.01 (-0.07 - 0.09) n= 10
BLACK SEA BS	180 \pm 47 177 (99 - 268) n=9	13 \pm 3 12 (10 - 20) n= 9	7.5 \pm 2.3 7.3 (4.8 - 11) n=9	-0.98 \pm 0.17 -0.94 (-1.41 - -0.85) n= 9	0.17 \pm 0.05 0.18 (0.10 - 0.24) n= 9	0.02 \pm 0.03 0.03 (-0.05 - 0.04) n= 9	0.09 \pm 0.04 0.08 (0.05 - 0.17) n= 9	-0.04 \pm 0.08 -0.04 (-0.12 - 0.07) n= 9
NORTHERN ADRIATIC SEA NAS	1714 \pm 1255 1174 (884 - 4432) n= 8	1160 \pm 883 877 (506 - 3115) n= 8	67 \pm 8.1 66 (54 - 8) n= 8	-0.01 \pm 0.14 -0.05 (-0.17 - 0.27) n= 8	0.54 \pm 0.13 0.59 (0.37 - 0.69) n= 8	0.01 \pm 0.04 0.02 (-0.07 - 0.07) n= 8	0.40 \pm 0.09 0.42 (0.29 - 0.50) n= 8	0.01 \pm 0.21 0.07 (-0.41 - 0.26) n= 8
RIA DE AVEIRO REFERENCE RAR	1368 \pm 804 1274 (333 - 2243) n= 6	737 \pm 431 887 (227 - 1122) n= 5	27 \pm 21 20 (10 - 50) n=3	-0.09 \pm 0.14 -0.13 (-0.23 - 0.11) n= 6	0.42 \pm 0.10 0.41 (0.29 - 0.55) n= 6	0.01 \pm 0.03 0.00 (-0.03 - 0.06) n= 6	0.33 \pm 0.10 0.31 (0.19 - 0.46) n= 6	0.13 \pm 0.21 0.20 (-0.17 - 0.34) n= 6
RIA DE AVEIRO CONTAMINATED RAC	2888 \pm 468 2785 (2309 - 3515) n= 10	1088 \pm 680 1220 (119 - 1903) n= 10	69 \pm 7 67 (57 - 80) n= 9	0.11 \pm 0.10 0.12 (-0.13 - 0.22) n= 10	0.20 \pm 0.07 0.19 (0.03 - 0.30) n= 10	0.002 \pm 0.02 0.01 (-0.03 - 0.03) n= 10	0.14 \pm 0.05 0.14 (0.05 - 0.21) n= 10	-0.17 \pm 0.15 -0.18 (-0.33 - 0.20) n= 10

785

Contamination levels and habitat use influence Hg accumulation and stable isotopes in the European seabass

Dicentrarchus labrax.

Marianna Pinzone^{a*}, Alice Cransveld^{a*}, Emmanuel Tessier^b, Sylvain Bérail^b, Joseph Schnitzler^{a,c}

Krishna Das^a, David Amouroux^b.

*Both authors contributed equally to the work

^aFreshwater and Oceanic sciences Unit of reSearch (FOCUS), Laboratory of Oceanology, University of Liège B6c Allée du 6 Août, 4000 Liège, Belgium

^bUniversité de Pau et des Pays de l'Adour, E2S UPPA, CNRS, Institut des Sciences Analytiques et de Physico-chimie pour l'Environnement et les matériaux (IPREM). Technopôle Helioparc, 2 Avenue Pierre Angot, 64053 Pau Cedex 09, France

^cInstitute for Terrestrial and Aquatic Wildlife Research, University of Veterinary Medicine Hannover, Foundation, 25761 Büsum, Schleswig-Holstein, Germany.

Highlights

- Isotopic ratios trace Hg organotropism and sources in the European seabass;
- We measured $\Delta^{199}\text{Hg}$ and $\delta^{202}\text{Hg}$ values, T-Hg and %MeHg in seabass muscle and liver;
- Our results suggest the occurrence of *in vivo* MeHg demethylation in seabass liver;
- In polluted areas inter-organs MDF gets masked by Hg saturation in fish tissues;
- In unpolluted sites, Hg MDF and MIF trace short-term shifts in fish habitat use.

Declaration of interests

The authors declare that they have no known competing financial interests or personal relationships that could have appeared to influence the work reported in this paper.

The authors declare the following financial interests/personal relationships which may be considered as potential competing interests:

Journal Pre-proof